Computational Mechanics 25 (2000) 448–455 © Springer-Verlag 2000

Numerical treatment of generalized plasticity with anisotropic elastic range in the case of plane stress

C. Huettel, A. Matzenmiller

Abstract The generalized plasticity model as presented by Lubliner (1991) and applied by Taylor and Auricchio (1995) is an extension of classical rate independent plasticity with a yield surface. For the generalized plasticity concept in Huettel and Matzenmiller (1999a) an integration algorithm under the restrictions of plane stress is presented that reduces the discretized tensor equations in the case of isotropy even for nonlinear hardening to the solution of a single scalar equation, as it is typical for the classical J_2-plasticity model in the complete three-dimensional case.

1 Introduction

The generalized plasticity model, as presented by Lubliner in Auricchio et al. (1992), Lubliner (1991) and Lubliner et al. (1993) is a generalization of classical rate-independent plasticity with a yield surface. This material model is able to describe a reloading transient during the reloading process, which is shown in the asymptotic approach of the reloading curve to the initial load curve in the stress-strain diagram, as observed in Lubhahn et al. (1961) for copper or in Greenstreet et al. (1973) for graphite. An advantageous extension of the generalized plasticity model to finite plastic strain regimes, which comprises classical plasticity and the model in Auricchio et al. (1995) for linear kinematic and isotropic hardening rules as special cases, is given in Huettel et al. (1999a).

In contrast to classical plasticity, where the yield function must vanish identically during plastic loading (see Schreyer et al. 1979), non-zero values of the yield criterion f are allowed in generalized plasticity. Following this new concept, the yield function may be regarded as an additional internal variable besides the plastic strains and the hardening variables, such as the backstresses and the plastic arclength.

In Schreyer et al. (1979) and Simo et al. (1988) a return mapping algorithm for plane stress elastoplasticity is given, which applies to isotropic as well as orthotropic linear elasticity relations between the stresses and the elastic strains. For this algorithm a constant value of the yield function, e.g. $f = 0$, in the case of plastic flow is essential, so that it does not apply to generalized plasticity. In Steinmann et al. (1997) and Huettel et al. (1999b) methods for enforcing the plane stress condition in a weak sense for arbitrary finite strain 3D-material models are derived. In the present paper an algorithm for small strain generalized plasticity is presented, which enforces the plane stress condition exactly.

The constitutive equations of the generalized plasticity concept in plane stress are introduced in Sect. 2. The classical elastoplastic tangent moduli, consistent with the continuous time constitutive equations are adressed. The numerical time integration of the constitutive equations is outlined in Sect. 3 and leads to a system of fifteen algebraic equations for the fifteen unknowns. In Sect. 4 the stresses are computed after the system of algebraic constitutive equations is reduced to the solution of two coupled nonlinear scalar equations in two unknowns. In the case of isotropy the algorithm may be further simplified to the solution of only one scalar equation as shown in Sect. 5. The tangent operator, consistent with the stress computation algorithm of Sect. 4, is given in the Appendix. It becomes the classical elastoplastic tangent moduli as the time increment approaches zero, which demonstrates the consistency of the algorithm in Sect. 4 with the continuous time model of Sect. 2. The paper finishes with some numerical examples.

2 Constitutive equations

The constitutive equations are briefly discussed in incremental notation for generalized plasticity in the following. The strain tensor is additively split into an elastic and a plastic part:

$$\mathrm{d}\{\mathbf{E}\} = \mathrm{d}\{\mathbf{E}_e\} + \mathrm{d}\{\mathbf{E}_p\} \ . \tag{1}$$

The subscripts e and p indicate elastic and plastic strains. The curly brackets are used for vector notation of the independent components of second order tensors in plane stress, e.g. $\{\mathbf{E}\} = [E_{11}, E_{22}, E_{12}]^{\mathrm{T}}$, with stress components $T_{13} = T_{23} = T_{33} \equiv 0$ and out of plane base vector $\mathbf{e}_3$. The stress tensor depends only on the elastic strains

$$\mathrm{d}\{\mathbf{T}\} = \mathbf{C}\mathrm{d}\{\mathbf{E}_e\} \ , \tag{2}$$

where $\mathbf{C}$ is the elasticity tensor in plane stress – see for example Eq. (32). The plastic strains change only in the case of plastic loading according to the normality rule

$$\mathrm{d}\{\mathbf{E}_p\} = \begin{cases} \mathrm{d}\lambda\{\mathbf{N}\} & : \text{for plastic loading} \\ \{\mathbf{0}\} & : \text{otherwise} \end{cases} , \tag{3}$$

where $\mathrm{d}\lambda$ is the incremental plastic multiplier and

$$\mathbf{N} = \frac{\partial f}{\partial \mathbf{T}} = \frac{(\mathbf{T} - \mathbf{X})^D}{\|(\mathbf{T} - \mathbf{X})^D\|} \tag{4}$$

Received 27 October 1999

C. Huettel (✉), A. Matzenmiller
Universitaet GH Kassel, Institute for Mechanics, Moenchebergstr. 7, D-34109 Kassel, Germany

is the normal to the yield surface, defined below, with $(\cdot)^D$ as the operator for the deviator of a tensor. Equation (5) represents the nonlinear Armstrong and Frederick type evolution equation of the back stresses $\mathbf{X}$ with parameters b and c:

$$\mathrm{d}\{\mathbf{X}\} = c\,\mathrm{d}\{\mathbf{E}_p\} - b\{\mathbf{X}\}\mathrm{d}s \ . \tag{5}$$

Equation (6) defines the plastic arclength s, computed from

$$\mathrm{d}s = \sqrt{\frac{2}{3}}\|\mathrm{d}\mathbf{E}_p\| = \begin{cases} \sqrt{\frac{2}{3}}\mathrm{d}\lambda : & \text{for plastic loading} \\ 0 \quad : & \text{otherwise} \end{cases} , \tag{6}$$

where use is made of Eqs. (3), (4). Equation (7) introduces the nonlinear isotropic hardening variable $k(s)$ with material parameters k_0, k_∞ and α:

$$k(s) = k_\infty + (k_0 - k_\infty)\mathrm{e}^{-\alpha s} \ . \tag{7}$$

The out-of-plane normal components E_{33}, X_{33} and N_{33} of the tensors $\mathbf{E}$, $\mathbf{X}$ and $\mathbf{N}$ are dependent variables: the component E_{e33} follows from the plane stress condition, E_{p33}, X_{33} and N_{33} from the deviatoric property of $\mathbf{E}_p$, $\mathbf{X}$ and $\mathbf{N}$ due to the von Mises plastic potential, i.e. $\mathrm{tr}(\mathbf{E}_p) = 0$ and finally $E_{33} = E_{e33} + E_{p33}$.

The yield function is of the von Mises type:

$$f(\mathbf{T}, \mathbf{X}, s) = \|(\mathbf{T} - \mathbf{X})^D\| - \sqrt{\tfrac{2}{3}}k(s) \gtrless 0 \ .$$

In contrast to the theory of classical plasticity the yield function f is treated as an additional constitutive variable, since positive values of the yield function are allowed during plastic loading. If the yield function f is negative, the stress state lies inside the elastic domain. If the stress increment $\mathrm{d}\mathbf{T}$ points inward with respect to the yield surface (see Fig. 1), elastic unloading takes place.

Accordingly, the loading conditions read:

$$f < 0 \quad \text{or} \quad \mathbf{N} \cdot \mathrm{d}\mathbf{T} \leq 0 \rightarrow \text{elastic behaviour}$$
$$f \geq 0 \quad \text{and} \quad \mathbf{N} \cdot \mathrm{d}\mathbf{T} > 0 \rightarrow \text{plastic loading.}$$

An additional constitutive equation, the so-called limit equation – see Eq. (8a), is introduced to determine the evolution of the yield function f in the case of plastic loading. The limit equation in Auricchio et al. (1995) is modified to account for strain history effects and, simultaneously, to simplify it for the numerical time integration – see Huettel et al. (1999a):

$$\mathrm{d}F = h(f)\mathrm{d}f - g(s)\mathrm{d}s \equiv 0 \tag{8a}$$

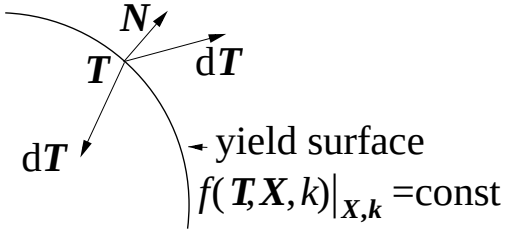

Fig. 1. Yield surface with normal $\mathbf{N}$ and stress increments $\mathrm{d}\mathbf{T}$

The functions $h(f)$ and $g(s)$ are specified as follows:

$$h(f) = \frac{\delta f}{f_\infty - f} \quad \text{and} \quad g(s) = 1/\sqrt{s} \ , \tag{8b}$$

where δ and f_∞ are material parameters. Classical plasticity is recovered as a special case, if $h(f) \equiv 1$ and $g(s) \equiv 0$.

The elastoplastic tangent moduli are derived by introducing the matrix $\mathbf{B}$ for the calculation of the scalar product of two deviatoric tensors in plane stress, e.g. $\mathbf{N}$ and $\mathbf{X}$, written in vector notation as $\{\mathbf{N}\}$ and $\{\mathbf{X}\}$:

$$\mathbf{N} \cdot \mathbf{X} := \mathrm{tr}(\mathbf{N}^{\mathrm{T}}\mathbf{X}) = \{\mathbf{N}\}^{\mathrm{T}}\mathbf{B}\{\mathbf{X}\}$$
$$\rightarrow \quad \mathbf{B} := \begin{bmatrix} 2 & 1 & 0 \\ 1 & 2 & 0 \\ 0 & 0 & 2 \end{bmatrix} ,$$

where $\mathrm{tr}(\cdot)$ is the trace operator. The operator

$$\mathbf{P} = \frac{1}{3}\begin{bmatrix} 2 & -1 & 0 \\ -1 & 2 & 0 \\ 0 & 0 & 3 \end{bmatrix}$$

extracts the stress deviator from the stress tensor: $\mathbf{P}\{\mathbf{T}\} = \{\mathbf{T}^D\}$. Using Eqs. (2), (1) and (3), the scalar product of $\mathrm{d}\mathbf{T}$ with the deviatoric tensor $\mathbf{N}$ yields in vector notation to:

$$\mathbf{N} \cdot \mathrm{d}\mathbf{T} = \{\mathbf{N}\}^{\mathrm{T}}\mathbf{B}\mathbf{P}\mathrm{d}\{\mathbf{T}\}$$
$$= \{\mathbf{N}\}^{\mathrm{T}}\mathbf{B}\mathbf{P}\mathbf{C}\mathrm{d}\{\mathbf{E}\} - \mathrm{d}\lambda\{\mathbf{N}\}^{\mathrm{T}}\mathbf{B}\mathbf{P}\mathbf{C}\{\mathbf{N}\} \ . \tag{9}$$

The scalar product of $\mathrm{d}\mathbf{X}$ with $\mathbf{N}$ reads due to Eqs. (5) and (3):

$$\{\mathbf{N}\}^{\mathrm{T}}\mathbf{B}\mathrm{d}\{\mathbf{X}\} = \left[c - \sqrt{\tfrac{2}{3}}b(\mathbf{N} \cdot \mathbf{X})\right]\mathrm{d}\lambda \tag{10}$$

The differential of the yield function $\mathrm{d}f$ may be expressed with Eqs. (9), (10) and (4):

$$\mathrm{d}f = \left[\sqrt{\tfrac{2}{3}}b(\mathbf{N} \cdot \mathbf{X}) - c - \{\mathbf{N}\}^{\mathrm{T}}\mathbf{B}\mathbf{P}\mathbf{C}\{\mathbf{N}\} - \sqrt{\tfrac{2}{3}}k'(s)\right]\mathrm{d}\lambda$$
$$+ \{\mathbf{N}\}^{\mathrm{T}}\mathbf{B}\mathbf{P}\mathbf{C}\mathrm{d}\{\mathbf{E}\} \ , \tag{11}$$

where $k'(s) = \frac{\mathrm{d}k(s)}{\mathrm{d}s}$. Substitution of $\mathrm{d}f$ and Eq. (6) into the limit Eq. (8a) gives the incremental plastic multiplier:

$$\mathrm{d}\lambda = A_{GP}\{\mathbf{N}\}^{\mathrm{T}}\mathbf{B}\mathbf{P}\mathbf{C}\mathrm{d}\{\mathbf{E}\} \tag{12}$$

with

$$A_{GP} = \frac{h(f)}{h(f)\left[\{\mathbf{N}\}^{\mathrm{T}}\mathbf{B}\mathbf{P}\mathbf{C}\{\mathbf{N}\} + c - \sqrt{\tfrac{2}{3}}b(\mathbf{N} \cdot \mathbf{X}) + \sqrt{\tfrac{2}{3}}k'(s)\right] + \sqrt{\tfrac{2}{3}}g(s)} \ .$$

Finally, substituting Eq. (12) in Eq. (3) leads with the aid of Eqs. (1) and (2) to the elastoplastic tangent

$$\mathbf{C}_{GP} := \frac{\mathrm{d}\{\mathbf{T}\}}{\mathrm{d}\{\mathbf{E}\}} = \mathbf{C} - A_{GP}\mathbf{C}\{\mathbf{N}\}\mathbf{B}\mathbf{P}\{\mathbf{N}\}^{\mathrm{T}}\mathbf{C} \ , \tag{13}$$

where use has been made of the fact that $\mathbf{BP}$ is a diagonal matrix. The elastoplastic tangent is symmetric, regardless

of the applied hardening rule. Equation (13) comprises the case of classical plasticity, where $h(f) \equiv 1$ and $g(s) \equiv 0$.

3
Numerical time integration of constitutive equations

For the time discretization of the rate equations in Sect. 2, the differentials $\mathrm{d}(\cdot)$ turn into increments $\Delta(\cdot)$. From the known process variables $\mathbf{u}^n$, $\mathbf{E}_p^n$, $\mathbf{X}^n$, $\mathbf{T}^n$, s^n and f^n in the equilibrium configuration at time t^n, their new values at t^{n+1} have to be calculated for a given displacement increment $\Delta\mathbf{u} = {}^i\mathbf{u} - \mathbf{u}^n$ in the context of standard finite element procedures. The strain increment $\{\Delta\mathbf{E}\}$ is obtained from the incremental displacement by:

$$\{\Delta\mathbf{E}\} = \left[\frac{\partial\Delta u_1}{\partial x_1}, \frac{\partial\Delta u_2}{\partial x_2}, \frac{1}{2}\left(\frac{\partial\Delta u_1}{\partial x_2} + \frac{\partial\Delta u_2}{\partial x_1}\right)\right]^{\mathrm{T}} .$$

The stresses ${}^i\mathbf{T}$ at time t^{n+1} are then calculated from the strain increment $\Delta\mathbf{E}$:

$$\begin{aligned}\{{}^i\mathbf{T}\} &= \mathbf{C}\{\mathbf{E}_e^n + \Delta\mathbf{E}_e\} = \mathbf{C}\{\mathbf{E}_e^n + \Delta\mathbf{E}\} - \mathbf{C}\{\Delta\mathbf{E}_p\} \\ &=: \{{}^{\mathrm{T}}\mathbf{T}\} - \mathbf{C}\{\Delta\mathbf{E}_p\} \ .\end{aligned}$$

$\{{}^{\mathrm{T}}\mathbf{T}\}$ are the *trial* stresses, resulting from the assumption that the material behaves elastically in the time interval considered. The supposition of purely elastic behaviour is confirmed, if

$${}^{\mathrm{T}}f := f({}^{\mathrm{T}}\mathbf{T}, \mathbf{X}^n, s^n) < 0 \quad \text{or} \quad {}^{\mathrm{T}}f \le f^n$$

holds. If elastic behaviour is ascertained, the stresses at time t^{n+1} are given by the trial stresses. If plastic loading occurs, an implicit Euler difference formula allows the update of the time dependent variables in incremental form:

$$\{{}^i\mathbf{E}_p\} = \{\mathbf{E}_p^n\} + \{\Delta\mathbf{E}_p\} = \{\mathbf{E}_p^n\} + \lambda\{\mathbf{N}\} \tag{14}$$

$$\{{}^i\mathbf{X}\} = \{\mathbf{X}^n\} + \{\Delta\mathbf{X}\} = V(\lambda)(\{\mathbf{X}^n\} + \lambda c\{\mathbf{N}\}) \tag{15}$$

$$\{{}^i\mathbf{T}\} = \{{}^{\mathrm{T}}\mathbf{T}\} - \lambda\mathbf{C}\{\mathbf{N}\} \tag{16}$$

$$\{\mathbf{N}\} = \{({}^i\mathbf{T} - {}^i\mathbf{X})^D\}/\|({}^i\mathbf{T} - {}^i\mathbf{X})^D\| \tag{17}$$

$${}^is = s^n + \Delta s = s^n + \sqrt{\frac{2}{3}}\lambda \tag{18}$$

$${}^if = \|({}^i\mathbf{T} - {}^i\mathbf{X})^D\| - \sqrt{\frac{2}{3}}k({}^is) \tag{19}$$

$$0 = H({}^if) - H(f^n) - G({}^is) + G(s^n) \ , \tag{20}$$

where

$$V(\lambda) := \left(1 + \sqrt{\tfrac{2}{3}}b\lambda\right)^{-1} \tag{21}$$

and $\Delta\lambda$ is replaced by λ for notational simplicity. The functions

$$H(f) = \int h(f)\mathrm{d}f = -\delta\left[f + f_\infty \ln\left(1 - \frac{f}{f_\infty}\right)\right] + \mathrm{C}_h$$

and

$$G(s) = \int g(s)\mathrm{d}s = 2\sqrt{s} + \mathrm{C}_g$$

are the integrals of $h(f)$ and $g(s)$ in Eq. (8b) with arbitrary integration constants C_h and C_g.

4
Plasticity with anisotropic elastic range

The system with fifteen linear and nonlinear algebraic Eqs. (14)–(20) is efficiently solved by reducing it to two scalar equations. For this purpose the relative stress deviator $\{({}^i\mathbf{T} - {}^i\mathbf{X})^D\}$ is written as:

$$\begin{aligned}\{({}^i\mathbf{T} - {}^i\mathbf{X})^D\} = \mathbf{P}\{{}^{\mathrm{T}}\mathbf{T}\} - \mathbf{V}(\lambda)\{\mathbf{X}^{\mathbf{n}}\} - \lambda\mathbf{PC}\{\mathbf{N}\} \\ - c\lambda V(\lambda)\{\mathbf{N}\} \ ,\end{aligned} \tag{22}$$

after use has been made of Eqs. (15) and (16). By the aid of the definition

$$\{\boldsymbol{\Theta}\} := \mathbf{P}\{{}^{\mathrm{T}}\mathbf{T}\} - V(\lambda)\{\mathbf{X}^n\} \tag{23}$$

Equation (22) may be recast into:

$$\{({}^i\mathbf{T} - {}^i\mathbf{X})^D\} = \{\boldsymbol{\Theta}\} - \lambda\mathbf{PC}\{\mathbf{N}\} - c\lambda V(\lambda)\{\mathbf{N}\} \ . \tag{24}$$

Adding the zero vector $\beta\{\mathbf{N}\} - \beta\{\mathbf{N}\}$ to the right hand side of Eq. (24), where β is at this stage an arbitrary scalar, and defining

$$\{\boldsymbol{\Xi}\} := \{\boldsymbol{\Theta}\} + (\beta\mathbf{1} - \lambda\mathbf{PC})\{\mathbf{N}\} \ , \tag{25}$$

the final form of the relative stress deviator follows as:

$$\{({}^i\mathbf{T} - {}^i\mathbf{X})^D\} = \{\boldsymbol{\Xi}\} - [\beta + c\lambda V(\lambda)]\{\mathbf{N}\} \ . \tag{26}$$

In the case of an isotropic elasticity relation between the stresses and the elastic strains a special choice for the scalar β allows for further simplification – see Sect. 5. Here it is sufficient to take $\beta = 0$. From Eqs. (17), (23) and (26) it becomes obvious that the tensors $\mathbf{N}$, $\boldsymbol{\Theta}$ and $\boldsymbol{\Xi}$ are all deviatoric, so that the quantity $\mathbf{PC}\{\mathbf{N}\}$ in Eq. (25) must be a deviatoric tensor too.

Since the normal $\{\mathbf{N}\}$ points in the direction of the relative stress deviator $\{({}^i\mathbf{T} - {}^i\mathbf{X})^D\}$, the quantity $\{\boldsymbol{\Xi}\}$ also is proportional to $\{\mathbf{N}\}$, according to Eq. (26), and equal to its definition in Eq. (25):

$$\{\boldsymbol{\Xi}\} = \|\boldsymbol{\Xi}\|\{\mathbf{N}\} = \{\boldsymbol{\Theta}\} - \lambda\mathbf{PC}\{\mathbf{N}\} \tag{27}$$

$$\Rightarrow \ \{\mathbf{N}\} = \mathbf{R}\{\boldsymbol{\Theta}\} \tag{28}$$

$$\Rightarrow \ 1 = \{\boldsymbol{\Theta}\}^{\mathrm{T}}\mathbf{R}^{\mathrm{T}}\mathbf{BR}\{\boldsymbol{\Theta}\} \ , \tag{29}$$

where

$$\mathbf{R} = \hat{\mathbf{R}}(\|\boldsymbol{\Xi}\|, \lambda) = (\lambda\mathbf{PC} + \|\boldsymbol{\Xi}\|\mathbf{1})^{-1}$$

and $\|\mathbf{N}\| = 1$ are used in Eq. (29). The yield function in Eq. (19) reduces to

$${}^if(\|\boldsymbol{\Xi}\|, \lambda) = \|\boldsymbol{\Xi}\| - c\lambda V(\lambda) - \sqrt{\tfrac{2}{3}}k({}^is) \tag{30}$$

after use is made of Eqs. (26) and (27). ${}^if(\|\boldsymbol{\Xi}\|, \lambda)$ and Eq. (18) are inserted into Eq. (20) to derive besides Eq. (29) a second scalar equation for $\|\boldsymbol{\Xi}\|$ and the plastic rate parameter λ:

$$H[{}^if(\|\boldsymbol{\Xi}\|, \lambda)] - H(f^n) - G[{}^is(\lambda)] - G(s^n) = 0 \ . \tag{31}$$

The system of equations in Sect. 3 is reduced to the solution of the two nonlinear Eqs. (29), (31) for the two unknowns $\|\boldsymbol{\Xi}\|$ and λ, which may be found iteratively, e.g.

by Newton's method. Once λ and $\|\boldsymbol{\Xi}\|$ are known, $\{\mathbf{N}\}$ and $\{{}^{i}\mathbf{T}\}$ may be computed from Eqs. (28) and (16) successively.

The problem in Sect. 3 may be further simplified to the solution of only one scalar equation.

1. In the case of classical plasticity, where $H(f) = f$ and $G(s) = 0$. Equation (31) reduces to the condition ${}^{i}f(\|\boldsymbol{\Xi}\|, \lambda) = f^{n}$, which renders $\|\boldsymbol{\Xi}\|$ to be an explicit function of λ in face of Eq. (30). The right hand side of the remaining Eq. (29) then depends only on λ.
2. In the case of an isotropic elasticity relation between the stresses and the elastic strains, as shown next.

5 Isotropic elasto-plasticity with isotropic elasticity

For isotropic elasticity and plane stress

$$\mathbf{C} = \frac{E}{1-v^2}\begin{bmatrix} 1 & v & 0 \\ v & 1 & 0 \\ 0 & 0 & 1-v \end{bmatrix} \tag{32}$$

is the elasticity tensor, E is Young's modulus and v Poisson's ratio. The system of Eqs. (14)–(20) may be reduced to a single scalar equation for the solution. With regard to Eq. (25) one may easily verify the notation in components of the expression

$$(2G\mathbf{1} - \mathbf{PC})\{\mathbf{N}\} = -\frac{E(1-2v)}{3(1-v^2)} N_{33}[1 \quad 1 \quad 0]^{\mathrm{T}} \ , \tag{33}$$

where G is the shear modulus. By setting $\beta = 2G\lambda$, Eq. (25) takes a particularly simple form

$$\{\boldsymbol{\Xi}\} = \{\boldsymbol{\Theta}\} - m\lambda N_{33}\{\mathbf{M}\} \ , \tag{34}$$

with

$$m := \frac{E(1-2v)}{3(1-v^2)}$$

and

$$\{\mathbf{M}\} := [1 \quad 1 \quad 0]^{\mathrm{T}} \ .$$

From Eqs. (17), (15), (23) and (26) it is obvious that $\mathbf{N}$, $\boldsymbol{\Theta}$ and $\boldsymbol{\Xi}$ represent all deviatoric tensors, so that $\mathbf{M}$ in Eq. (34) must be a deviatoric tensor too, i.e

$$M_{33} = -M_{11} - M_{22} = -2 \ .$$

As stated in Sect. 4, $\{\boldsymbol{\Xi}\}$ is proportional to $\{\mathbf{N}\}$:

$$\{\boldsymbol{\Xi}\} = \|\boldsymbol{\Xi}\|\{\mathbf{N}\} \ , \tag{35}$$

which together with Eq. (34) for the out-of-plane normal component yields:

$$\Xi_{33} = \|\boldsymbol{\Xi}\| N_{33} = \Theta_{33} + 2m\lambda N_{33}$$

$$\Leftrightarrow \quad N_{33} = \frac{\Theta_{33}}{\|\boldsymbol{\Xi}\| - 2m\lambda} \ . \tag{36}$$

Hence, Eq. (34) becomes:

$$\{\boldsymbol{\Xi}\} = \{\boldsymbol{\Theta}\} - m\lambda \frac{\Theta_{33}}{\|\boldsymbol{\Xi}\| - 2m\lambda}\{\mathbf{M}\} \ . \tag{37}$$

The Euclidean norm $\|\boldsymbol{\Xi}\|$ of the second order deviatoric tensor $\boldsymbol{\Xi}$ is computed from Eq. (37) by $\|\boldsymbol{\Xi}\|^2 = \{\boldsymbol{\Xi}\}^{\mathrm{T}}\mathbf{B}\{\boldsymbol{\Xi}\}$, leading to a rational function $p(\|\boldsymbol{\Xi}\|)$, of which the coefficients depend on λ:

$$p(\|\boldsymbol{\Xi}\|) := p_1(\|\boldsymbol{\Xi}\|) - p_2(\|\boldsymbol{\Xi}\|) = 0 \tag{38}$$

$$p_1(\|\boldsymbol{\Xi}\|) := \|\boldsymbol{\Xi}\|^2 - \|\boldsymbol{\Theta}\|^2 \tag{39}$$

$$p_2(\|\boldsymbol{\Xi}\|) := \frac{6m\lambda\Theta_{33}^2(\|\boldsymbol{\Xi}\| - m\lambda)}{(\|\boldsymbol{\Xi}\| - 2m\lambda)^2} \ . \tag{40}$$

The roots of the function $p(\|\boldsymbol{\Xi}\|)$ are the intersections of the two functions $p_1(\|\boldsymbol{\Xi}\|)$ and $p_2(\|\boldsymbol{\Xi}\|)$. The graphs of the functions $p_1(\|\boldsymbol{\Xi}\|)$ and $p_2(\|\boldsymbol{\Xi}\|)$ are depicted in Fig. 2 for the special values of $\|\boldsymbol{\Theta}\| = 10$ MPa, $\Theta_{33} = 7.7$ MPa and $m\lambda = 2$ MPa.

The parameter b is taken as $b = 0$, so that $\{\boldsymbol{\Theta}\}$ is independent of λ. The yield function in Eq. (19) reduces to

$${}^{i}f = \|\boldsymbol{\Xi}\| - [2G + cV(\lambda)]\lambda - \sqrt{\frac{2}{3}}k({}^{i}s) \tag{41}$$

after use is made of Eqs. (26), (35) and $\beta = 2G\lambda$. Since the yield function ${}^{i}f$ is positive in the case of plastic flow, the following estimation holds:

$$\begin{aligned} \|\boldsymbol{\Xi}\| &\geq [2G + cV(\lambda)]\lambda + \sqrt{\frac{2}{3}}k({}^{i}s) \\ &= 2m\lambda + [2(G-m) + cV(\lambda)]\lambda + \sqrt{\frac{2}{3}}k({}^{i}s) \\ &= 2m\lambda + \left[\frac{E}{3(1-v)} + cV(\lambda)\right]\lambda + \sqrt{\frac{2}{3}}k({}^{i}s) \\ &> 2m\lambda \ . \end{aligned}$$

If $\|\boldsymbol{\Xi}\| > 2m\lambda > 0$, the function in Eq. (39) increases strictly monotonously, whereas the one in Eq. (40) decreases monotonously as

$$\frac{\partial p_2}{\partial\|\boldsymbol{\Xi}\|} = \frac{-6m\lambda\Theta_{33}^2\|\boldsymbol{\Xi}\|}{(\|\boldsymbol{\Xi}\| - 2m\lambda)^3}$$

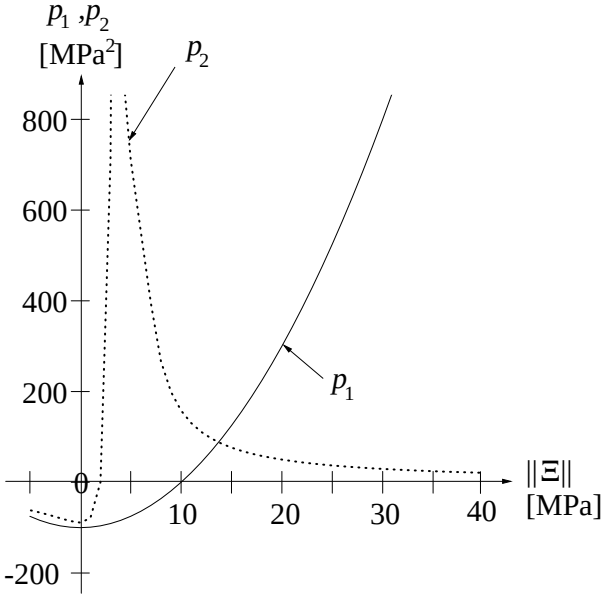

Fig. 2. Typical graphs

shows. Therefore, $p_1(2m\lambda) < p_2(2m\lambda) = +\infty$ and $p_1(2m\lambda + \|\boldsymbol{\Theta}\|) \geq p_2(2m\lambda + \|\boldsymbol{\Theta}\|)$ enforce the existence of one and only one intersection of p_1 and p_2 with $\|\boldsymbol{\Xi}\| > 2m\lambda$. The last estimation $p_1(2m\lambda + \|\boldsymbol{\Theta}\|) \geq p_2(2m\lambda + \|\boldsymbol{\Theta}\|)$ follows from $\|\boldsymbol{\Theta}\| > 0$ due to the definition in Eq. (23) in the case of plastic flow and $\Theta_{33}^2 \leq 2/3\|\boldsymbol{\Theta}\|^2$:

$$\frac{2}{3} \geq \frac{\Theta_{33}^2}{\|\boldsymbol{\Theta}\|^2}$$

$$\rightarrow \quad 4m\lambda(\|\boldsymbol{\Theta}\| + m\lambda) \geq \frac{6m\lambda\Theta_{33}^2(\|\boldsymbol{\Theta}\| + m\lambda)}{\|\boldsymbol{\Theta}\|^2}$$

$$\rightarrow \quad p_1(2m\lambda + \|\boldsymbol{\Theta}\|) \geq p_2(2m\lambda + \|\boldsymbol{\Theta}\|) \ .$$

$\Theta_{33}^2 \leq 2/3\|\boldsymbol{\Theta}\|^2$ in turn may be verified by maximizing $\Theta_{33}^2 = (\Theta_{11} + \Theta_{22})^2$ under the constraint $\|\boldsymbol{\Theta}\|^2 = \{\boldsymbol{\Theta}\}^{\mathrm{T}}\mathbf{B}\{\boldsymbol{\Theta}\}$ with the help of the Lagrange-multiplier method. Equation (38) may be multiplied with $(\|\boldsymbol{\Xi}\| - 2m\lambda)^2 > 0$ to gain the quartic polynomial

$$p_4(\|\boldsymbol{\Xi}\|) := (\|\boldsymbol{\Xi}\|^2 - \|\boldsymbol{\Theta}\|^2)(\|\boldsymbol{\Xi}\| - 2m\lambda)^2 - 6m\lambda\Theta_{33}^2(\|\boldsymbol{\Xi}\| - m\lambda) = 0 \ , \tag{42}$$

which possesses up to four real roots. The aforementioned derivations indicate that the correct root of this polynomial is the only one with $\|\boldsymbol{\Xi}\| > 2m\lambda$.

Equation (42) may be solved by means of Cardano's formula, giving $\|\boldsymbol{\Xi}\|$ as an explicit function of λ. Thus, the yield function in Eq. (41) also depends on λ only. ${}^{i}f(\lambda)$ and Eq. (18) may be inserted into Eq. (20) to derive a single scalar equation for the plastic rate parameter λ:

$$H[{}^{i}f(\lambda)] - H(f^n) - G[{}^{i}s(\lambda)] - G(s^n) = 0 \tag{43}$$

Solving Eq. (43) iteratively by Newton's method necessitates the prior choice of an initial value $\lambda_0 \geq 0$, such that $f(\lambda_0) < f_\infty$. However, in the examples below Eq. (42) was not solved by means of Cardano's formula, but iteratively by Newton's method.

In the special case ${}^{i}f = 0$ of classical plane stress plasticity the scalar $\|\boldsymbol{\Xi}\|$ is an explicit function of λ due to Eq. (41):

$$\|\boldsymbol{\Xi}\| = [2G - cV(\lambda)]\lambda + \sqrt{\frac{2}{3}}k({}^{i}s) \ .$$

Then, λ is obtained iteratively from Eq. (42) after $\|\boldsymbol{\Xi}\|$ is inserted. Once λ and $\|\boldsymbol{\Xi}\|$ are known, $\{\boldsymbol{\Xi}\}$, $\{\mathbf{N}\}$ and $\{{}^{i}\mathbf{T}\}$ may be computed from Eqs. (37), (35) and (16) successively.

The consistent tangent operator, obtained by linearization of the algorithm, is given in the Appendix.

6 Examples

The limit Eq. (8a) is rearranged to give:

$$f'(f,s) := \frac{\partial f}{\partial s} = \frac{g(s)}{h(f)} = \frac{f_\infty - f}{\delta f\sqrt{s}} \tag{44}$$

As observed in Eq. (44), the function $g(s)$ governs together with $h(f)$ the growth of the yield function, depending on the plastic arclength. Clearly, $g(s)$ increases or reduces the change $f'(f,s)$ of the yield function during plastic flow for small or large values of the plastic arclength. Since $f'(f,s)$ tends to infinity for $f = 0$, the elastoplastic stress-strain curve is continuous with its first derivative at the transition point between the elastic and the plastic domain. The case $f'(f,s) = 0$ may be viewed as stationary with respect to plastic deformations. The stationary state is approached as either f tends to f_∞ or s tends to ∞. Thus, f_∞ is the maximum value, which is reached by the yield function in the limit. The parameter δ is a measure for the rate of convergence of f to its limit f_∞.

Table 1. Specification of the two models

Reference	Symbol	$h(f)$	$g(s)$	δ
Auricchio et al. (1995)	A – – –	$\frac{\delta f}{f_\infty - f}$	const	0.0035
Huettel et al. (1999b)	B –––	$\frac{\delta f}{f_\infty - f}$	const/$\sqrt{s}$	0.0314

The stress algorithm in Sect. 5 together with the consistent tangent operator, given in the Appendix, were implemented into the finite element program FEAP (Zienkiewicz et al. 1989). The following examples shall illustrate the performance of the model and the algorithm.

Example 1: Unloading and reloading of tension specimen

The first example shows the influence of the function $g(s)$.

The performance of the model is demonstrated by means of a force driven tensile test, where repeated loading, unloading and reloading occur. The stress-strain diagram is depicted in Fig. 3. The parameter δ of model B is chosen such that the two curves in Fig. 3 fit together between the first and the second unloading. It may be observed that the generalized plasticity model describes a reloading transient during the reloading process, which is shown in the asymptotic approach of the reloading curve to the initial load curve. As already mentioned above, this feature demonstrates the special capability of generalized

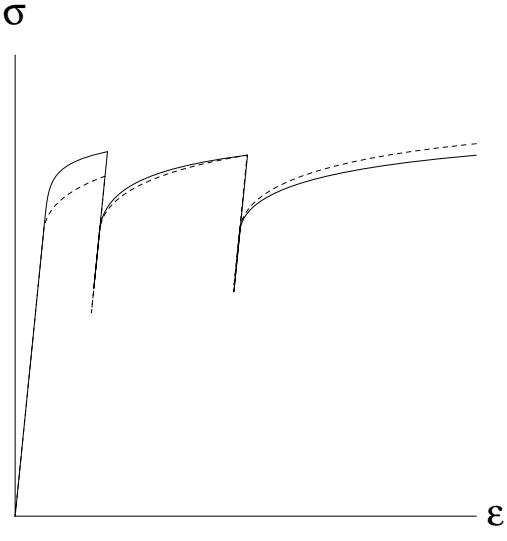

Fig. 3. Force driven interrupted uniaxial tensile test. $E = 10000$ MPa, $\nu = 0.3$, $k_0 = 15$ MPa, $k_\infty = 16$ MPa, $\alpha = 0.1$, $f_\infty = 10$ MPa, $c = b = 0$

Table 2. Parameters of the two models

Reference	Symbol	c (MPa)	b	δ
Auricchio et al. (1995)	A – – –	2000	0	0.0007
Huettel et al. (1999b)	B ——	10000	800	0.03

Table 3. Material parameters

E	ν	c	b	k_0	k_∞	α	δ	f_∞
10000 MPa	0.3	500 MPa	40	5 MPa	30 MPa	0.1	0.03	40 MPa

plasticity. Material model B renews plasticity more and more slowly as the plastic strain increases. In the case of small plastic strains it gives a higher uniaxial stress response than material model A. This shows that the function $g(s)$ is well suited to effectively control the dependency of the slope of the reloading curve in terms of the amount of prestrain.

Example 2: Cyclic plasticity

The second example shows the necessity to account for nonlinear kinematic hardening in generalized plasticity, if the uniaxial equivalent stresses are bounded. The functions $h(f)$ and $g(s)$ are the same as in the previous example. Since the model in Auricchio et al. (1995) does not include nonlinear kinematic hardening, it cannot describe hysteresis loops with horizontal asymptotes. This is in contrast to the proposed concept in Huettel et al. (1999b), as may be seen from the stress-strain diagram in Fig. 4. The parameter *delta* of model B is chosen such that the stress at the beginning of the first unloading is identical to that of model A. The other parameters are selected in order to point out the crucial effect and do not necessarily correspond to a real material data.

Example 3: Plane stress perforated tension strip

A tension strip with a circular hole is subjected to a constant surface load on two opposite sides. Due to the symmetry of the boundary value problem, only a quarter of the tension strip is analyzed. The dimensions and the boundary conditions of the tension strip are given in Fig. 5 and its discretization with 133 bilinear 4-node continuum elements in Fig. 6. The material parameters of the model in Huettel et al. (1999b) were set as follows:

The surface load was applied in nine steps. Maximum strains of $\varepsilon_{xx} = 16.5\%$ and maximum stresses of $\sigma_{xx} = 93$ MPa occurred at the end of loading. The deformed and undeformed mesh is plotted in Fig. 6. Plastified elements are drawn with solid lines, whereas elastic regions have thin element borders. The quadratic convergence to the solution in the last load step is shown in the table below.

The convergence criterion is the norm of out-of-balance forces during iteration. The example shows the excellent numerical performance of the model even in the case of multiaxial stress states.

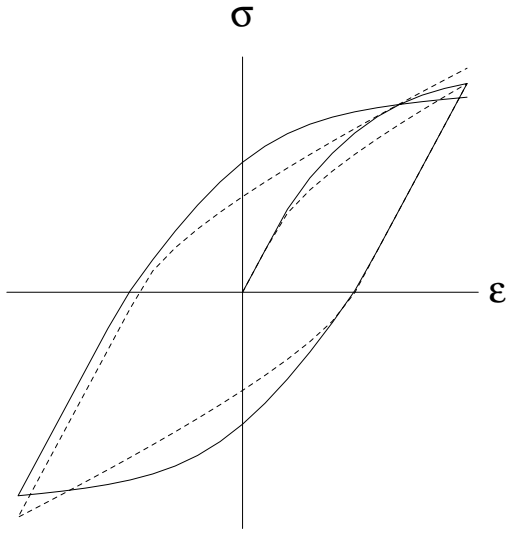

Fig. 4. Displacement driven uniaxial cyclic test. $E = 10000$ MPa, $\nu = 0.3$, $k_0 = 15$ MPa, $\alpha = 0$, $f_\infty = 30$ MPa

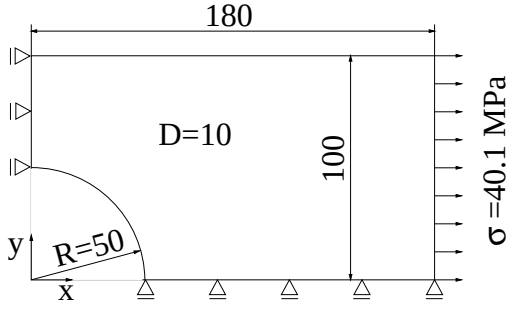

Fig. 5. Boundary conditions of the tension strip

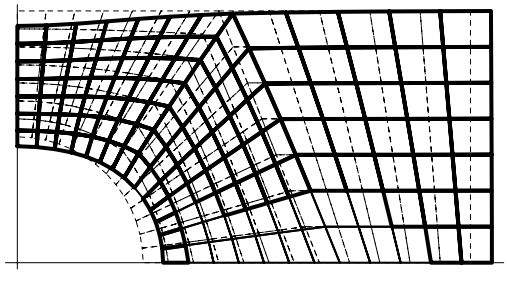

Fig. 6. Deformed and undeformed configuration

7 Summary

The generalized plasticity model allows room for the reloading transient. The constitutive equations of general-

Table 4. Convergence behaviour

Iteration	1	2	3	4	5	6	7
Criterion	0.5369	4.188	0.6994	0.02234	3.335E-05	1.119E-10	1.001E-21

ized plasticity are applied to plane stress conditions with a modification of the so called limit equation. The numerical solution scheme, employed for the constitutive equations, falls into the class of return mapping algorithms. Basically, the system of the constitutive equations reduces to the solution of a single scalar equation with one unknown. The tangent operators, consistent with the continuous time model and the stress computation algorithm is addressed. As expected, the tangent operator, following from the discrete time model, reduces to that of the continuous time model as the time increment approaches zero. The algorithm also applies to classical plasticity as a special case of generalized plasticity. The implementation of the return mapping algorithm into the finite element program FEAP is straight-forward. The performance of the model and the algorithm is examined using three numerical examples. They clearly demonstrate the applicability of the solution algorithm even for complex boundary value problems.

Appendix

Consistent tangent operator

The consistent tangent operator may be derived by linearization of the algorithm in Sect. 5. It guarantees the asymptotic quadratic convergence for the iterative solution of the displacement equations from standard finite element analysis. Omitting lengthy calculations, only a few substeps of the derivation are sketched.

The abbreviation $D(\cdot)(\{\Delta\mathbf{E}\})[\{\mathbf{H}\}] = D(\cdot)$ is used for the Gateaux differentials. For example, the differentials of the trial stresses $\{^{\mathrm{T}}\mathbf{T}\}$ and the plastic arclength ^{i}s follow from their definitions in Sect. 3:

$$D\{^{\mathrm{T}}\mathbf{T}\} = \mathbf{C}\{\mathbf{H}\}$$
$$D^{i}s = \sqrt{\tfrac{2}{3}}D\lambda \ .$$

The differentials of the yield function ^{i}f, $\{\boldsymbol{\Theta}\}$, Θ_{33} and the quantities $\|\boldsymbol{\Xi}\|$, N_{33} as well as $\|\boldsymbol{\Theta}\|^2$ are computed successively from Eqs. (20), (23), $\Theta_{33} = -[1\ 1\ 0]\{\boldsymbol{\Theta}\}$, (41), (36) and $\|\boldsymbol{\Theta}\|^2 = \{\boldsymbol{\Theta}\}^{\mathrm{T}}\mathbf{B}\{\boldsymbol{\Theta}\}$ in dependence of $\{\mathbf{H}\}$ and $\mathrm{D}\lambda$. Using these differentials, Eq. (42) supplies the differential of the plastic rate parameter:

$$D\lambda = \lambda A_1\{\mathbf{M}\}^{\mathrm{T}}\{\mathbf{H}\} + \frac{A_{NL}}{\|\boldsymbol{\Theta}\|}\{\boldsymbol{\Theta}\}^{\mathrm{T}}\mathbf{BPC}\{\mathbf{H}\} \ ,$$

where

$$A_1 = \frac{EA_2}{3(1-\nu)A_3} \tag{45}$$

$$A_{NL} = \frac{2\|\boldsymbol{\Theta}\|}{A_3}(\|\boldsymbol{\Xi}\| - 2m\lambda)^2 \tag{46}$$

$$A_2 = -12m\Theta_{33}(\|\boldsymbol{\Xi}\| - m\lambda) \tag{47}$$

$$A_3 = A_4A_5 + A_6 - 2\sqrt{\frac{2}{3}}bV^2(\boldsymbol{\Theta}\cdot\mathbf{X}^n)(\|\boldsymbol{\Xi}\| - 2m\lambda)^2 + \sqrt{\frac{2}{3}}\,b\lambda A_2V^2X_{33}^n$$

$$A_4 = \sqrt{\frac{2}{3}}\frac{g(^{i}s)}{h(^{i}f)} + 2G + cV^2 + \frac{2}{3}k'(^{i}s)$$

$$A_5 = 2\|\boldsymbol{\Xi}\|(\|\boldsymbol{\Xi}\| - 2m\lambda)^2 + 2(\|\boldsymbol{\Xi}\|^2 - \|\boldsymbol{\Theta}\|^2) \times (\|\boldsymbol{\Xi}\| - 2m\lambda) - 6m\lambda\Theta_{33}^2 \tag{48}$$

$$A_6 = 6m^2\lambda\Theta_{33}^2 - 6m\Theta_{33}^2(\|\boldsymbol{\Xi}\| - m\lambda) - 4m(\|\boldsymbol{\Xi}\|^2 - \|\boldsymbol{\Theta}\|^2)(\|\boldsymbol{\Xi}\| - 2m\lambda) \tag{49}$$

The differentials of $\{\boldsymbol{\Xi}\}$, $\{\mathbf{N}\}$ and finally $\{^{i}\mathbf{T}\}$ may be constructed by means of

$$\text{Eq. (34)} \rightarrow D\{\boldsymbol{\Xi}\} = D\{\boldsymbol{\Theta}\} - m(D\lambda N_{33} + \lambda DN_{33})\mathbf{M}$$

$$\text{Eq. (35)} \rightarrow D\{\mathbf{N}\} = \frac{1}{\|\boldsymbol{\Xi}\|}(D\{\boldsymbol{\Xi}\} - D\|\boldsymbol{\Xi}\|\{\mathbf{N}\})$$

$$\text{Eq. (16)} \rightarrow D\{^{i}\mathbf{T}\} = \mathbf{C}\{\mathbf{H}\} - D\lambda\,\mathbf{C}\{\mathbf{N}\} - \lambda\mathbf{C}D\{\mathbf{N}\} =: {}^{i}\mathbf{C}_{NL}\{\mathbf{H}\} \ . \tag{50}$$

The tangent operator then follows from Eq. (50) as

$${}^{i}\mathbf{C}_{NL} = \mathbf{C}\left\{\left[\frac{\lambda m(N_{33} + \lambda A_8)}{\|\boldsymbol{\Xi}\|}\{\mathbf{M}\} - \sqrt{\frac{2}{3}}\frac{bV^2\lambda}{\|\boldsymbol{\Xi}\|}\{\mathbf{X}^n\} - \left(1 - \frac{\lambda A_4}{\|\boldsymbol{\Xi}\|}\right)\{\mathbf{N}\}\right]\cdot\left[\lambda A_1\{\mathbf{M}\}^{\mathrm{T}} + \frac{A_{NL}}{\|\boldsymbol{\Theta}\|}\{\boldsymbol{\Theta}\}^{\mathrm{T}}\mathbf{BPC}\right] - \frac{\lambda}{\|\boldsymbol{\Xi}\|}\mathbf{PC} + \frac{\lambda^2 mA_7}{\|\boldsymbol{\Xi}\|}\{\mathbf{M}\}\{\mathbf{M}\}^{\mathrm{T}}\right\} + \mathbf{C} \ , \tag{51}$$

where

$$A_7 = \frac{-E}{3(1-\nu)(\|\boldsymbol{\Xi}\| - 2m\lambda)}$$

$$A_8 = \sqrt{\frac{2}{3}}\frac{bV^2X_{33}^n}{\|\boldsymbol{\Xi}\| - 2m\lambda} - \frac{\Theta_{33}(A_4 - 2m)}{(\|\boldsymbol{\Xi}\| - 2m\lambda)^2} \tag{52}$$

For $\Delta t \rightarrow 0$, and therefore also $\lambda \rightarrow 0$, it is shown that the consistent tangent operator reduces to the classical tangent operator $\mathbf{C}_{GP}$ in Sect. 2, i.e. $\lim_{\lambda\rightarrow 0}\mathbf{C}_{NL} = \mathbf{C}_{GP}$. Firstly, it may be observed that for $\lambda \rightarrow 0$

$$\{\boldsymbol{\Xi}\} = \{\boldsymbol{\Theta}\}$$
$$\{\mathbf{N}\} = \{\boldsymbol{\Theta}\}/\|\boldsymbol{\Theta}\|$$

follows from Eqs. (34) and (35). Equation (51) then implies that the tangent operator reduces for $\lambda \rightarrow 0$ to

$${}^{i}\mathbf{C}_{NL} = \mathbf{C} - A_{NL}\mathbf{C}\{\mathbf{N}\}\{\mathbf{N}\}^{\mathrm{T}}\mathbf{BPC} \ .$$

From Eqs. (21), (36), (48), (49) and (46) follows together with the identity $3mN_{33}^2 = \{\mathbf{N}\}^{\mathrm{T}}\mathbf{BPC}\{\mathbf{N}\} - 2G$:

$$V = (1 + \sqrt{\tfrac{2}{3}}b\lambda)^{-1} = 1$$
$$A_5 = 2\|\boldsymbol{\Theta}\|^3$$
$$A_6 = -2\|\boldsymbol{\Theta}\|^3(2G - \{\mathbf{N}\}^{\mathrm{T}}\mathbf{BPCN})$$
$$\rightarrow \ A_{NL} = A_{GP}$$

Hence, $\lim_{\lambda\rightarrow 0}\mathbf{C}_{NL} = \mathbf{C}_{GP}$, which was to be shown.

References

Auricchio F, Taylor RL, Lubliner J (1992) Application of a Return Map Algorithm to Plasticity Models. In: Owen DRJ, Onate E, (eds.) COMPLAS Computational Plasticity: Fundamentals and Applications, Barcelona, 2229

Auricchio F, Taylor RL (1995) Two material models for cyclic plasticity: nonlinear kinematic hardening and generalized plasticity. Int. J. Plasticity 11(1): 65–98

Greenstreet WL, Phillips A (1973) A theory of an elastic-plastic continuum with special emphasis to artificial graphite. Acta Mechanica 16: 143–156

Huettel C, Matzenmiller A (1999a) Consistent discretization of thickness strains in thin shells including 3D-material models. Commun. Num. Meth. Eng. 15: 283–293

Huettel C, Matzenmiller A (1999b) Extension of generalized plasticity to finite deformations and non-linear hardening. Int. J. Solids Struct. 36: 5255–5276

Lubhahn JD, Felger RP (1961) Plasticity and Creep of Metals. Wiley, New York

Lubliner J (1991) A simple model of generalized plasticity. Int. J. Solids Struct. 28(6): 769–778

Lubliner J, Taylor RL, Auricchio F (1993) A new model of generalized plasticity and its numerical implementation. Int. J. Solids Struct. 30(22): 3171–3184

Schreyer HL, Kulak RL, Kramer JM (1979) Accurate numerical solutions for elastic-plastic models. J. Pressure Vessel Tech. 101: 226–234

Simo JC, Govindjee S (1988) Exact closed-form solution of the return mapping algorithm in plane stress elastoplasticity. Eng. Comput. 5: 254–258

Steinmann P, Betsch P, Stein E (1997) FE plane stress analysis incorporating arbitrary 3D large strain constitutive models. Eng. Comput. 14(2): 175–201

Zienkiewicz OC, Taylor RL (1989) The finite element method, 4th edn, McGraw-Hill Book Company, London